JCTC Journal of Chemical Theory and Computation

Article

pubs.acs.org/JCTC

Multiconfiguration Pair-Density Functional Theory: Barrier Heights and Main Group and Transition Metal Energetics

Rebecca K. Carlson, Giovanni Li Manni, Andrew L. Sonnenberger, Donald G. Truhlar,* and Laura Gagliardi*

Department of Chemistry, Chemical Theory Center, and Supercomputing Institute, University of Minnesota, Minneapolis, Minnesota 55455, United States

Supporting Information

ABSTRACT: Kohn−Sham density functional theory, resting on the representation of the electronic density and kinetic energy by a single Slater determinant, has revolutionized chemistry, but for open-shell systems, the Kohn−Sham Slater determinant has the wrong symmetry properties as compared to an accurate wave function. We have recently proposed a theory, called multiconfiguration pair-density functional theory (MC-PDFT), in which the electronic kinetic energy and classical Coulomb energy are calculated from a multiconfiguration wave function with the correct symmetry properties, and the rest of the energy is calculated from a density functional, called the on-top density functional, that depends on the density and the on-top pair density calculated from this wave function. We also proposed a simple way to approximate the on-top density functional by translation of Kohn−Sham exchange-correlation functionals. The method is much less expensive than other post-SCF methods for calculating the dynamical correlation energy starting with a multiconfiguration self-consistent-field wave function as the reference wave function, and initial tests of the theory were quite encouraging. Here, we provide a broader test of the theory by applying it to bond energies of main-group molecules and transition metal complexes, barrier heights and reaction energies for diverse chemical reactions, proton affinities, and the water dimerization energy. Averaged over 56 data points, the mean unsigned error is 3.2 kcal/mol for MC-PDFT, as compared to 6.9 kcal/mol for Kohn−Sham theory with a comparable density functional. MC-PDFT is more accurate on average than complete active space second-order perturbation theory (CASPT2) for main-group small-molecule bond energies, alkyl bond dissociation energies, transition-metal−ligand bond energies, proton affinities, and the water dimerization energy.

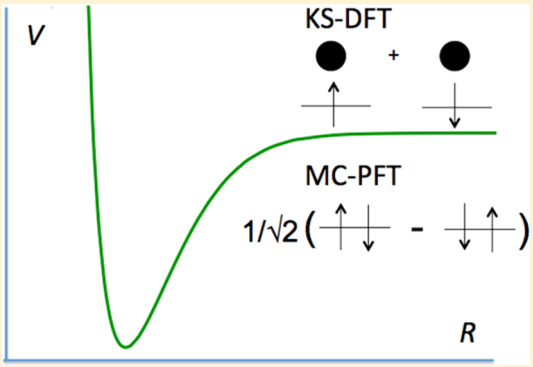

1. INTRODUCTION

Wave function theory (WFT) and density functional theory (DFT) have complementary strengths for electronic structure problems. Great progress has been made in the ability of theory to make useful predictions of barrier heights, bond energies, complexation energies, and other quantities important for mechanistic, analytical, and synthetic chemistry.[1,2] However, problem areas remain, one of which is the treatment of strongly correlated systems, which may also be described as inherently multiconfiguration systems. Such systems, sometimes called multireference systems (in contrast to weakly correlated systems, which may also be called single-reference systems and which are described qualitatively correctly by a single electronic configuration) include many transition metal complexes, some transition states, systems with partially broken bonds, and most electronically excited states.

For treating inherently multiconfigurational systems, WFT methods such as complete active space self-consistent field theory (CASSCF)[3] or other multiconfiguration self-consistent-field (MCSCF) methods[4] have the advantage of explicitly describing the dominant electron configurations, but they do not include enough dynamical correlation energy to be quantitatively accurate. More quantitative results for dissociation energies, barrier heights, and excitation energies of both main group and transition-metal containing systems can be produced when wave functions obtained by these methods are used as reference wave functions for post-SCF dynamical correlation treatments such as complete active space second order perturbation theory (CASPT2)[5] or multireference configuration interaction (MRCI).[6] MCSCF methods with smaller configuration spaces, such as generalized valence bond,[7] restricted active space self-consistent field theory (RASSCF),[8] occupation-restricted-multiple-active space (ORMAS) SCF method,[9] generalized active space self-consistent field theory (GASSCF),[10] and SplitGAS,[11] have also been used successfully to model multireference systems. However, adding the rest of the correlation energy to an MCSCF calculation by post-SCF wave function methods has the major drawback that computational cost rises rapidly as system size increases.

Received: September 10, 2014

DOI: 10.1021/ct5008235
J. Chem. Theory Comput. XXXX, XXX, XXX−XXX

Because the electron−electron interaction is a two-body operator, the electronic energy can be written exactly in terms of the one-particle and two-particle density matrices. The Hohenberg−Kohn theorem shows that the energy is also a functional of the one-particle density, which leads to DFT.[12] Density functional theory in the Kohn−Sham formulation (KS-DFT)[13] can treat much larger systems than dynamically correlated WFT. Although KS-DFT uses a single configurational representation of the density, it would be an exact theory if the exact exchange-correlation functional were used. However, the exact functional is unknown and probably unknowable. With the use of existing functionals, the treatment of strongly correlated systems is much less satisfactory than the treatment of weakly correlated ones.[14] First of all, one must use spin-polarized (spin-unrestricted) density functional theory in which the energy is a functional of the spin densities (spin-up and spin-down densities) rather than the total density, which is their sum. Not only are the energies less accurate but the theory becomes ambiguous as to which state is being approximated because the stationary solutions of the Kohn−Sham equation do not have the correct symmetry properties.[15]

Recently, we published a new method that combines the strengths of WFT and DFT in a new theory, called multiconfigurational pair-density functional theory (MC−PDFT).[16] This theory is not covered by the Hohenberg−Kohn theorem because it involves the diagonal element of the two-particle density matrix (but not the whole two-particle density matrix); we call the diagonal element of the two-particle density matrix the on-top density. The on-top density offers a way to treat inherently multiconfigurational systems with the correct symmetry,[17−20] and MC-PDFT uses new on-top density functionals to create a systematic new density functional method. The first step in this theory is a correlated WFT calculation, which we have so far taken to be an MCSCF calculation and in particular a CASSCF calculation. There have been many previous attempts to combine MCSCF theory with DFT, but these have been plagued with the problem of double counting portions of the correlation energy.[21] We eliminated this problem by calculating only the kinetic energy from the CASSCF wave function; all other components of the energy are calculated in a post-SCF step by a functional of the (one-particle) density and the on-top pair density calculated from the CASSCF wave function. Because the MC-PDFT method is systematic, it offers a clear path forward for improvements. Another appealing aspect of MC-PDFT is that its computational cost scales with system size in the same way as CASSCF (the cost depends on the choice of active space), but we are aiming at producing results similar to (and eventually better than) CASPT2 quality, without the added expense of CASPT2

As already mentioned, MC-PDFT requires a new kind of density functional, called the on-top density functional, which is a functional of the total density and the on-top density rather than of the spin densities on which the exchange-correlation functionals of spin-polarized Kohn−Sham theory depend. For our first applications, we developed on-top density functionals by a simple translation protocol that we postulated for converting a generalized-gradient-approximation (GGA) exchange-correlation functional to an on-top density functional; we calculated 19 atomic and molecular excitation energies (the molecules have 2−11 atoms) and six diatomic potential energy curves and dissociation energies (four for main-group diatomics and two for diatomics containing a transition metal), and we obtained encouraging results.[16] For example, MC-PDFT provided a realistic description of the potential energy curve of the dissociating N_2 molecule, which transforms upon dissociation from a closed-shell singlet to a system with six unpaired electrons.

To further develop the theory, we need improvements in three regards: (i) We need to understand the performance of MC-PDFT for a broader class of problems, including barrier heights and a more representative set of transition metal bond energies. (ii) We need to identify or develop less expensive methods than CASSCF for determining the kinetic energy, density, and on-top density. CASSCF, although much less expensive than CASPT2 or MRCI, is still prohibitively expensive when large active spaces are required to model the chemical problem of interest. (iii) We need to develop more accurate on-top density functionals.

We need to carry out step i before we can carry out step ii because we need to establish more broadly than was done in our initial paper, how well the theory works with CASSCF wave functions. They provide a systematic standard when they are affordable, so that we can see how much accuracy, if any, is lost when using simpler methods to generate the kinetic energy, density, and on-top density. That is the goal of the present paper, in which we continue to use CASSCF with one of our simple translated functionals, in particular, tPBE[16] (which is a translation of the PBE[22] functional for the MC−PDFT method). We report the results of MC−PDFT over a broader set of data than in the original paper, in particular, we consider six main-group atomization energies for systems with 2−12 atoms, ten transition-metal atomization energies for systems with 2−6 atoms, three proton affinities of triatomic and tetra-atomic molecules, two alkyl bond dissociation energies for systems with 17 and 18 atoms, the complexation energy of the water dimer, 24 barrier heights for reactions with 3−7 atoms, and 10 energies of reaction for the subset of these reactions where the energy of reaction is not zero. This makes a total of 56 data points, and the database may be called CE56 (denoting 56 chemical energies).

In addition to comparing the MC-PDFT results to reference data derived mainly from experiment, we also compare to conventional Kohn−Sham calculations with three standard exchange-correlation functionals, namely, the PBE[22] GGA and two hybrid functionals, B3LYP,[23−26] and M06-2X.[27] We note that the M06-2X functional, when originally published,[27] was recommended only for systems that do not contain transition metals, but it is applied here to the entire database just to illustrate the difficulty in Kohn−Sham theory of obtaining excellent performance for transition metals with one of the best functionals for the main group.

The theory was presented in the original paper[16] and is summarized in Section 2. Section 3 explains the CE56 database.

2. THEORY

A detailed description of the theory can be found in our previous paper,[16] but we summarize the main points here. Using a nonrelativistic, Born−Oppenheimer Hamiltonian, the usual energy expression for a multiconfiguration electronic wave function is given by

$$E = V_{nn} + \sum_{pq} h_{pq} D_{pq} + \frac{1}{2} \sum_{pqrs} g_{pqrs} d_{pqrs} \tag{1}$$

where V_{nn} is the sum of nuclear−nuclear repulsion terms, h_{pq} and g_{pqrs} are the one-electron and two-electron integrals,

DOI: 10.1021/ct5008235
J. Chem. Theory Comput. XXXX, XXX, XXX−XXX

respectively, and D_{pq} and d_{pqrs} are the one- and two-body electronic density matrices, respectively. The indices p, q, r, and s refer to generic orbitals. By distinguishing between inactive orbitals (doubly occupied in all configurations generated by the CASSCF wave function, indices i and j) and active orbitals (indices v, w, x, and y), the energy expression simplifies to

$$E = V_{\mathrm{nn}} + 2\sum_{i} h_{ii} + \sum_{ij}(2g_{iijj} - g_{ijij}) + \sum_{vw} h_{vw}D_{vw} + \sum_{ivw}(2g_{iivw} - g_{iviw})D_{vw} + \frac{1}{2}\sum_{vwxy} g_{vwxy}d_{vwxy} \quad (2)$$

In MC−PDFT energy, we replace eq 2 with

$$E = V_{\mathrm{nn}} + 2\sum_{i} h_{ii} + 2\sum_{ij} g_{iijj} + \sum_{vw} h_{vw}D_{vw} + 2\sum_{ivw} g_{iivw}D_{vw} + \frac{1}{2}\sum_{vwxy} g_{vwxy}D_{vw}D_{xy} + E_{\mathrm{ot}}[\rho, \Pi] \quad (3)$$

where $E_{\mathrm{ot}}[\rho, \Pi]$ is the on-top density functional of the total density ρ and on-top pair density Π. The difference between eq 2 and eq 3 is in that the two-electron contribution has been replaced by a Coulomb term involving the product of one-body density matrices and a functional of the total density and on-top density.

3. CE56 DATABASE AND ITS SUBDATABASES

All data in the energetic databases are nonrelativistic electronic energies (including nuclear repulsion for molecules). For values derived from experiment, the rotational−vibrational and zero-point energies and the spin−orbit energy have been removed from experimental values as described in detail in previous work.[28] For databases based on atomization energies, we divide the atomization energy by the number of bonds in the molecule to produce the average bond energy for that molecule; in counting bonds, a double bond counts as one bond, that is, we add bonds, not bond orders. The reason for this is so that the large atomization energies of large molecules do not have an excessive effect on the mean errors. The seven subdatabases that compose the CE56 database are all based on previous work[14,28−38] and are explained in Table 1. The actual data in each database will be shown in Tables 2−8 later in the article.

4. COMPUTATIONAL DETAILS

One goal in developing the MC−PDFT method was to create a general method that describes a state with a well-defined wave function for any single-reference or multireference system and derives an energy from that wave function as a post-SCF step. By using a CASSCF wave function, a state with the correct symmetry of the wave function is unambiguously defined and is used to provide the kinetic energy, density, and on-top density for the post-SCF on-top density functional. For multireference systems, there is no longer a need to describe a state with a broken symmetry approach,[39−42] which is commonly used in KS−DFT.

All MC−PDFT, CASSCF, and CASPT2 calculations were performed with a locally modified version of the *Molcas* electronic structure package;[43] these methods will soon be available in an update to version 8. All calculations are nonrelativistic except when the Ag atom is present (see below), and geometries were obtained from the respective databases specified in Table 1 (see also Supporting Information). The basis sets used for the database containing transition metals were def2-TZVP[44] for metals and ma-TZVP[45] for other atoms. For Ag, the def2-TZVP relativistic effective core potential was used. Calculations for all other databases used the MG3S[46] basis set. Atomization energies are computed as the difference between the sum of the energies of the atoms and the energy of molecule.

Reasonable CASSCF active spaces were selected for each system. The active spaces are specified in the footnotes of the tables. In all cases, we use the same active space for CASSCF, CASPT2, and MC-PDFT.

All CASPT2 calculations were performed with standard imaginary shift[47] value of 5.44 eV and the *Molcas* default IPEA shift[48] of 6.80 eV. The imaginary shift serves to remediate the problem of intruder states, and the ionization-potential-electron-affinity (IPEA) shift is a parameter modifying the zeroth-order Hamiltonian that adjusts the energies of the active orbitals to be in better agreement with experiment. In the CASPT2 calculations, we did not correlate the core orbitals. For the main group we froze 1s orbitals; for the second period, we froze 1s, 2s, and 2p orbitals, except for Si for which we only froze 1s and 2s; for 3d transition metals we froze 1s, 2s, 2p, and 3s orbitals; and for Ag we froze 1s, 2s, 2p, 3s, 3p, 3d, and 4s orbitals.

The KS−DFT results presented for comparison were obtained from previous work.[38]

Table 1. Descriptions of Subdatabases

subdatabase	description
MGABE6	six main-group average bond energies. This database is obtained from an older database (AE6, from ref 29) of six atomization energies by dividing each datum by the number of bonds in the molecule.
TMABE10	10 average bond energies of molecules containing transition metals: reference data and geometry for AgH and FeH from ref 14, for CoH from ref 38, and for the other 7 from Zhang et al. (ref 28)
PA3	proton affinities of 3 small molecules from ref 31
ABDE2	two alkyl bond dissociation energies from refs 29, 32, and 33
WDCE1	water dimer complexation energy from ref 34
DBH24/08	24 diverse barrier heights from refs 29, 35, 36, and 37 (the "/08" denotes that we use the database as updated in 2008[37])
DRE10	10 diverse reaction energies from DBH24/10
MGE46	ten main-group energies, consisting of the union of MGABE6, PA3, ABDE2, WDCE1, DBH24/08, and DRE10

5. MULTIREFERENCE DIAGNOSTICS

In order to better understand the results, it is useful to have a quantitative measure of the multireference nature of each system in the database. While there are many diagnostics that have been used to define the extent of multireference character in a system,[49−67] we limit ourselves here to just two. In particular, we report both (i) the M diagnostic,[55] called M, which is derived from natural orbital occupation numbers of a CASSCF wave function, and (ii) the percentage weight of the dominant configuration from a CASSCF wave function, which is the absolute square of the largest coefficient in the configuration interaction expansion expressed as a percentage and is called P.

A rough rule of thumb is that a state is considered to have multireference character if $M \geq 0.04$ and/or $P \leq 95$. For atomization energies and bond dissociation energies, we use the full molecule to determine the M diagnostic (thus the diagnostics shown do not take account of the fact that the multireference character could be larger in the fragments produced by breaking bonds than in the parent molecule). For

DOI: 10.1021/ct5008235
J. Chem. Theory Comput. XXXX, XXX, XXX−XXX

Table 2. Main-Group Average Bond Energies (kcal/mol)

			WFT		MC-PDFT	KS-DFT			
	M^a	P^b	CASSCF	CASPT2	tPBE	PBE	M06-2X	B3LYP	exp.
SiH_4[c]	0.02	96.3	72.4	78.0	78.9	78.4	80.4	80.9	81.2
S_2[d]	0.07	94.8	76.9	100.8	109.2	114.7	104.2	102.9	104.3
SiO[e]	0.04	94.2	191.0	188.0	187.2	196.3	190.2	188.0	193.1
C_3H_4[f]	0.06	92.8	95.2	113.8	117.5	120.2	117.5	117.1	117.5
HC(O)CHO[g]	0.07	90.6	110.5	123.1	127.1	132.7	126.7	126.2	126.8
C_4H_8[h]	0.03	95.6	73.7	92.4	95.5	97.3	95.7	95.1	95.8
MUE			16.5	3.8	2.3	4.4	0.7	1.4	

[a]The M diagnostic values are computed according to ref 55. [b]The percent dominant configuration is of the CASSCF wave function. [c]The active space is 8/8, where the eight electrons are the σ bonding electrons and the eight orbitals are the σ bonding and antibonding orbitals. [d]The AS is 12/8, the full valence space, where the electrons and orbitals are the valence 3s and 3p choices. [e]The AS is 10/8, the full valence space, where the electrons and orbitals are the valence s and p choices for each atom. [f]The AS is 8/8 and excludes all carbon−hydrogen bonds. The eight electrons are those of the carbon−carbon triple bond and the carbon−carbon single bond. The orbitals are the corresponding bonding and antibonding pairs. [g]The AS is 12/12 and includes the carbon atomic 2p electrons and orbitals and the oxygen 2p electrons and orbitals. [h]The AS is 8/8, where the electrons and orbitals are bonding electrons of the carbon−carbon single bonds and the orbitals are the corresponding bonding/antibonding pairs.

Table 3. Transition-Metal−Ligand Average Bond Energies (kcal/mol)

			WFT		MC-PDFT	KS-DFT			
	M^a	P^b	CASSCF	CASPT2	tPBE	PBE	M06-2X	B3LYP	exp.
AgH[c]	0.05	97.7	38.2	52.2	52.9	55.9	48.1	54.5	54.0
FeH[d]	0.65	53.2	19.2	28.9	32.2	49.3	57.4	57.2	36.8
CoH[e]	0.98	34.4	18.2	42.9	39.8	60.5	56.5	60.1	45.2
TiCl[f]	0.05	50.0	92.3	104.2	103.6	116.6	97.9	103.8	102.3
CrCl[g]	0.01	99.4	64.0	86.4	82.3	89.8	99.1	86.7	91.0
VF_5[h]	0.06	89.7	74.2	107.6	116.9	126.5	103.1	111.8	113.4
$CrCl_2$[i]	0.006	99.5	72.5	80.7	78.2	88.8	96.6	85.3	91.4
MnF_2[j]	0.01	99.4	87.3	118.2	120.7	127.6	113.8	117.2	116.5
$FeCl_2$[k]	0.008	99.4	78.3	94.2	95.7	99.5	94.7	93.3	96.6
$CoCl_2$[l]	0.01	99.5	74.4	77.7	91.3	94.0	94.9	86.0	93.5
MUE			22.2	5.5	4.5	7.6	7.2	6.1	

[a]The M diagnostic values are computed according to ref 55. [b]The percent dominant configuration is of the CASSCF wave function. [c]The active space is 12/7, where the electrons and orbitals are those from the 4d and 5s orbitals of Ag and the 1s of hydrogen. The spin state is a singlet. [d]The AS is 9/7, where the electrons and orbitals are those from the 3d and 4s orbitals of Fe and the 1s orbital of hydrogen. The spin state is a quartet. [e]The AS is 10/7, where the electrons and orbitals are those from the 3d and 4s orbitals of Co and the 1s orbital of hydrogen. The spin state is triplet. [f]The AS is 5/7, where the electrons and orbitals are those from the 3d and 4s orbitals of Ti and the bonding 3p electron and orbital of Cl. The spin state is a quartet. [g]The AS is 7/7, where the electrons and orbitals are those from the 3d and 4s orbitals of Cr and the bonding 3p electron and orbital of Cl. The spin state is a sextet. [h]The AS is 10/11, where the electrons and orbitals are those from the 3d and 4s orbitals of V and the bonding 2p electron and orbital of each F. The spin state is a singlet. [i]The AS is 8/8, where the electrons and orbitals are those from the 3d and 4s orbitals of Cr and the bonding 3p electron and orbital of Cl. The spin state is a quartet. [j]The AS is 9/8, where the electrons and orbitals are those from the 3d and 4s orbitals of Mn and the bonding 2p electron and orbital of F. The spin state is a sextet. [k]The AS is 10/8, where the electrons and orbitals are those from the 3d and 4s orbitals of Fe and the bonding 3p electron and orbital of Cl. The spin state is a quintet. [l]The AS is 11/8, where the electrons and orbitals are those from the 3d and 4s orbitals of Co and the bonding 3p electron and orbital of Cl. The spin state is a quartet.

proton affinities and the hydrogen-bonded water dimer, we use the protonated species and the hydrogen-bonded complex as the measure of multireference character. Finally, for barrier heights and reaction energies, we use the transition state as the multireference measure.

6. RESULTS

Tables 2−8 give the results obtained with three standard KS−DFT functionals and with CASSCF, CASPT2, and MC−PDFT. These tables also give the active space specifications, using the notation n/m, where n is the number of active electrons, and m is the number of active orbitals. The bottom row of each table is the mean unsigned error averaged over the values in the table. Tables 2−8 also include the M and P diagnostics explained in Section 4. Table 9 contains the mean unsigned errors averaged over all 56 data, and it compares these to separate averages for the 10 data involving transition metals and the 46 data that do not involve transition metals. All mean errors in the tables are computed from unrounded data, not from the rounded data in the tables. The atomization energies underlying the data in Tables 2 and 3 are first converted to average bond energies, as listed in the tables, and the errors for each molecule and the mean errors are computed using the average bond energies.

7. DISCUSSION

CASPT2 is sensitive to the active space choice, in particular, to the size of the correlating space. The present active spaces are large enough to remove the major static correlation error in most cases, but the dynamical correlation, even the portion due only to the valence space, is very slowly convergent with respect to the size of the active space (the dynamical correlation energy is even more slowly convergent at the CASSCF level, such that CASSCF is not a practically useful method to recover

DOI: 10.1021/ct5008235
J. Chem. Theory Comput. XXXX, XXX, XXX−XXX

Table 4. Proton Affinities of Small Molecules (kcal/mol)

	M^a	P^b	CASSCF	CASPT2	tPBE	PBE	M06-2X	B3LYP	Exp.
NH_3[c]	0.02	96.3	212.9	212.3	212.1	210.9	209.9	211.3	211.9
H_2O[d]	0.02	97.4	171.0	171.5	172.3	170.4	170.7	170.5	171.8
H_2S[e]	0.03	96.2	188.6	174.9	174.0	174.4	172.4	174.8	173.7
MUE			5.5	0.6	0.3	1.03	1.4	1.03	

[a]The *M* diagnostic values are computed according to reference55. [b]The percent dominant configuration is of the CASSCF wave function. [c]The AS is 6/6. [d]The AS is 4/4. [e]The AS is 8/7, which includes the 3*s* and 3*p* electrons and orbitals from S and the 1*s* electrons and orbitals from each H, plus the orbital from the proton.

Table 5. Alkyl Bond Dissociation Energies (kcal/mol)

	M^a	P^b	CASSCF	CASPT2	tPBE	PBE	M06-2X	B3LYP	exp.
tBu-CH_3[c]	0.02	96.2	74.5	95.1	92.9	86.2	92.7	81.6	93.7
tBu-OCH_3[d]	0.03	98.9	70.3	93.0	89.6	80.1	89.9	76.2	89.3
MUE			19.1	2.6	0.5	8.3	0.8	12.6	

[a]The *M* diagnostic values are computed according to ref 55. [b]The percent dominant configuration is of the CASSCF wave function. [c]The AS is 8/8 for the molecule, which includes all carbon−carbon electrons and corresponding bonding/antibonding orbital pairs. For the methyl radical, the AS was 1/1. For the butyl radical, the AS was 7/7 for the butyl radical, which includes the carbon−carbon electrons and corresponding bonding/antibonding orbital pairs plus the radical electron and orbital. [d]The AS is 2/2 for the molecule, which includes all carbon−carbon electrons and corresponding bonding/antibonding orbital pairs. For each radical, the AS was 1/1.

Table 6. Noncovalent Energy of Hydrogen Bonding (kcal/mol)

	M^a	P^b	CASSCF	CASPT2	tPBE	PBE	M06-2X	B3LYP	exp.
$(H_2O)_2$[c]	0.02	96.0	4.0	5.5	4.8	5.4	5.5	4.96	4.97
unsigned error			0.96	0.5	0.2	0.5	0.5	0.01	

[a]The *M* diagnostic values are computed according to reference55. [b]The percent dominant configuration is of the CASSCF wave function. [c]The AS is 16/8 for the dimer, and 8/4 for each water molecule.

dynamical correlation energy). Chief among the questions that the present tests are designed to answer is "Are these reasonable active spaces large enough to yield accurate bond energies and barrier heights energies by MC-PDFT?".

Table 2 shows that CASSCF has a mean unsigned error (MUE) of 17 kcal/mol for main group bond energies. This is by far the largest error of the methods tested, as expected because it is the only method that does not attempt to recover the full or full valence dynamical correlation energy. Recovering more dynamical correlation energy with CASPT2 reduces the errors by more than a factor of 4, but only to 3.8 kcal/mol. In fact, for this test set, the errors for CASPT2 are almost as big as those for standard KS−DFT with the PBE functional (4.4 kcal/mol). The two hybrid functionals, M06-2X and B3LYP, have the lowest errors for the main group atomization energies at 0.7 and 1.4 kcal/mol, respectively. While MC−PDFT does not perform as well as these standard hybrid functionals; tPBE does improve by factors of 1.9 and 1.7 over PBE and CASPT2.

The *M* and *P* diagnostic values show that four of the systems in Table 1 (all except SiH_4 and C_4H_8) are multireference systems. The tPBE results are quite accurate for the two cases with the most multireference character, which is very encouraging for the ability of MC-PDFT to treat multireference systems.

Table 3 gives average bond energies of molecules containing transition metals, where the average bond energy is the atomization energy per bond (atomization energy divided by the number of bonds in the molecules). Table 3 shows that CASSCF tends to underestimate the atomization energy and has a mean unsigned error of 22.2 kcal/mol per bond. As for the main group atomization energies, CASPT2 reduces the average error as compared to CASSCF, in this case to 5.5 kcal/mol per bond. M06-2X is included in this table only for completeness because the original article[27] presenting it said it was not designed for treating transition metals; it has a mean unsigned error of 7.2 kcal/mol per bond. The other hybrid functional, B3LYP, has an average error of 6.1 kcal/mol, and PBE and tPBE have an average error of 7.6 and 4.5 kcal/mol, respectively.

For the three transition metal hydrides in Table 3 (rows 1−3), tPBE performs better than CASPT2. All three of these cases are considered to be multireference systems by the *M* and *P* diagnostics, but the weight of the dominant configuration is high for AgH.

The metal halides (rows 4−10 of Table 3) are not characterized as having significant multireference character by either diagnostic, except for VF_5 and TiCl. In some cases, such as $FeCl_2$ and $CoCl_2$, tPBE improves upon CASPT2 and does about as well as standard KS−DFT. In other cases like CrCl and $CrCl_2$, tPBE substantially underestimates the atomization energy.

Table 3 shows that for cases with a high *M* value and low dominant-configuration reference weight, tPBE generally does well. A particular success of tPBE compared with PBE is VF_5. With PBE, the atomization energy is about 66 kcal/mol too high (13 kcal/mol per bond), and tPBE reduces this error by almost a factor of 4.

In Table 4, we report proton affinities for three small molecules. All methods have lower average errors than CASSCF (5.5 kcal/mol). For this test set, tPBE has the lowest average error of 0.3 kcal/mol, followed by CASPT2 (0.6 kcal/mol). Standard KS−DFT has errors that are significantly higher (1.0−1.4 kcal/mol for the functionals tested here and about 2 kcal/mol for a typical exchange-correlation functional[38]). This is a very significant success for the new formalism since proton affinity is a direct test of the effect of changing the external

DOI: 10.1021/ct5008235
J. Chem. Theory Comput. XXXX, XXX, XXX−XXX

Table 7. Forward and Reverse Barrier Heights for Small Molecules (kcal/mol)

	M^a	P^b	CASSCF	CASPT2	tPBE	PBE	M06-2X	B3LYP	exp.
$OH + CH_4 \rightarrow H_2O + CH_3$	0.03	93.1	18.9	6.9	2.3	−5.2	5.4	2.3	6.5
reverse[c]			24.4	17.9	17.4	8.8	17.5	13.9	19.6
$H + HO \rightarrow H_2 + O$	0.04	96.5	17.1	12.0	10.7	3.6	9.6	4.0	10.5
reverse[d]			27.0	13.8	8.0	−1.3	11.8	6.3	12.9
$H + H_2S \rightarrow H_2 + HS$	0.04	96.0	11.3	5.5	4.2	−1.1	4.4	−0.5	3.5
reverse[e]			24.6	18.1	15.1	9.5	18.2	15.9	16.8
$H + N_2O \rightarrow OH + N_2$	0.08	87.6	29.8	20.4	17.3	10.5	17.6	11.8	17.1
reverse[f]			96.2	80.2	71.6	52.8	82.1	73.1	82.3
$H + ClH \rightarrow HCl + H$	0.05	95.8	29.9	20.4	16.5	10.4	18.6	13.1	18.0
reverse[g]			29.9	20.4	16.5	10.4	18.6	13.1	18.0
$CH_3 + FCl \rightarrow CH_3F + Cl$	0.09	91.7	8.3	8.9	6.3	−6.4	4.7	−1.5	6.8
reverse[h]			86.5	51.1	45.5	42.0	59.7	51.2	59.2
$Cl^-\cdots CH_3Cl \rightarrow ClCH_3\cdots Cl^-$	0.03	99.1	20.2	12.2	7.9	6.9	13.5	9.0	13.4
reverse[i]			20.2	12.2	7.9	6.9	13.5	9.0	13.4
$F^-\cdots CH_3Cl \rightarrow FCH_3\cdots Cl^-$	0.03	95.6	6.4	2.4	0.2	−1.0	3.2	0.1	3.4
reverse[j]			46.5	26.5	26.2	21.0	33.5	26.2	29.4
$OH^- + CH_3F \rightarrow HOCH_3 + F^-$	0.04	95.1	10.3	−3.6	−6.7	−10.7	−2.9	−5.9	−2.4
reverse[k]			30.6	17.2	14.1	9.6	17.5	14.6	17.7
$H + N_2 \rightarrow HN_2$	0.07	91.1	26.5	16.6	13.0	5.6	14.1	7.8	14.4
reverse[l]			−0.5	10.9	14.5	9.2	11.3	11.0	10.6
$H + C_2H_4 \rightarrow CH_3CH_2$	0.08	90.0	−9.6	1.7	3.4	0.0	2.9	−0.1	1.7
reverse[m]			34.5	41.3	43.0	40.4	43.7	41.9	41.8
$HCN \rightarrow HNC$	0.06	92.7	53.9	48.2	46.7	46.0	46.2	47.7	48.1
reverse[n]			37.5	33.9	32.8	41.0	33.3	33.8	32.8
MUE			10.2	1.7	3.2	8.5	0.98	4.2	

[a]The M diagnostic values are computed according to ref 55. [b]The percent dominant configuration is of the CASSCF wave function. [c]The AS for the transition state is 15/13. [d]The AS for the transition state is 8/6. [e]The AS for the transition state is 9/7. [f]The AS for the transition state is 17/13. [g]The AS for HCl is 8/5 which includes the valence electrons and orbitals on Cl and the 1s electron and orbital from H, 1/1 for hydrogen, and 9/6 for the transition state, which includes the aforementioned electrons and orbitals. [h]The AS for CH_3 is 7/7, which includes the carbon−hydrogen σ electrons and corresponding bonding/antibonding orbitals and the electron and orbitals of the radical. The AS for FCl is 10/6 which includes the valence p electrons and orbitals of the halogens. The AS for the TS is 17/13, the sum of the reactant active spaces. The AS for CH_3F is 12/10 which includes the carbon 2s and 2p electrons and orbitals, the fluorine 2p electrons and orbitals, and the hydrogen 1s electrons and orbitals. Finally, for Cl, the AS is 5/3 which includes the 3p electrons and orbitals. [i]The AS is 10/9 for all molecules, and includes the carbon−hydrogen σ bonds and corresponding bonding/antibonding orbitals, the bonding lone pair and orbital on the coordinating Cl, and the bonding electrons and corresponding bonding/antibonding orbitals of the bonded Cl. [j]The AS is 10/9 for all molecules, and is analogous to $Cl^-\cdots CH_3Cl \rightarrow ClCH_3\cdots Cl^-$. [k]The AS is 2/1 for the anions, corresponding to the electrons that will form the bond in the reaction. For the neutral species, the AS is 8/8 and includes all electrons and their corresponding bonding/antibonding orbitals that are associated with the central carbon atom. For the TS, the AS is analogous to $Cl^-\cdots CH_3Cl \rightarrow ClCH_3\cdots Cl^-$ and $F^-\cdots CH_3Cl \rightarrow FCH_3\cdots Cl^-$. [l]The AS is 1/1 for hydrogen and 10/8 for N_2 corresponding to the valence electrons and orbitals. The TS and HN_2 were described with an AS of 11/9, the sum of the active spaces used for the products. [m]The AS is 1/1 for hydrogen and 12/13 for C_2H_4. The TS and product both used an AS of 13/14. [n]The AS is 10/9 for all species, corresponding to the 1s electron and orbital of hydrogen and the valence 2s and 2p electrons and orbitals from carbons and nitrogen.

potential in which the electrons move without changing the number of electrons or their spin state.

Alkyl bond dissociation energies are well-known to be a difficult problem for Kohn−Sham DFT.[33,68−70] For alkyl bond dissociation energies, given in Table 5, tPBE has the lowest error of 0.5 kcal/mol, followed by M06-2X with an average error of 0.8 kcal/mol. The CASPT2 error is much smaller than CASSCF (2.6 vs 19.1 kcal/mol, respectively) and the popular B3LYP functional has an error of 12.6 kcal/mol.

For the noncovalent energy of hydrogen bonding in a water dimer, given in Table 6, B3LYP is the best method tested with an error of 0.01 kcal/mol, followed by tPBE with an error of 0.2 kcal/mol. The other functionals and CASPT2 give a much higher error of 0.5 kcal/mol.

In Table 7, we test the new theory against a diverse set of forward and reverse barrier heights for chemical reactions.[37] M06-2X has the lowest mean unsigned error (1.0 kcal/mol), followed by CASPT2 (1.7 kcal/mol). Comparing tPBE to PBE, the average error is reduced by a factor of 2.7 (3.2 vs 8.5 kcal/mol). As is typical of CASSCF, the average error is the highest (10.2 kcal/mol) of any of the methods tested, and B3LYP has an average error of about 4 kcal/mol, which is typical behavior for this functional.[36,37] Comparing PBE and tPBE, we see that when PBE predicts an incorrect sign of either the forward or reverse barrier height (which is the case for the first, second, sixth and eighth reactions in the table), tPBE instead gets the correct sign. For the sixth reaction, whose transition structure has the highest multireference character of any reaction considered, PBE underestimates the barrier height by 13.2 kcal/mol for the forward barrier, while tPBE predicts the correct sign and only underestimates the barrier by 0.5 kcal/mol. The fourth and 11th reactions are the next highest in multireference character by both diagnostics. For the former, tPBE outperforms PBE and is better than CASPT2 for describing the forward barrier. For the latter, CASPT2 is very accurate; the performance of tPBE is very similar to M06-2X for this reaction although the forward barrier height is overestimated. In general, for the reactions in Table 7, tPBE

DOI: 10.1021/ct5008235
J. Chem. Theory Comput. XXXX, XXX, XXX−XXX

Table 8. Reaction Energies for Small Molecules (kcal/mol)[a]

	CASSCF	CASPT2	tPBE	PBE	M06-2X	B3LYP	exp.
$OH + CH_4 \rightarrow H_2O + CH_3$	−5.5	−11.0	−15.2	−14.0	−12.1	−11.5	−13.1
$H + HO \rightarrow H_2 + O$	−10.0	−1.8	2.7	4.9	−2.2	−2.3	−2.4
$H + H_2S \rightarrow H_2 + HS$	−13.3	−12.6	−10.9	−10.6	−13.7	−16.4	−13.3
$H + N_2O \rightarrow OH + N_2$	−66.4	−59.8	−54.4	−42.4	−64.5	−61.3	−65.1
$CH_3 + FCl \rightarrow CH_3F + Cl$	−78.2	−42.2	−39.2	−48.4	−55.0	−52.8	−52.4
$F^-\cdots CH_3Cl \rightarrow FCH_3\cdots Cl^-$	−40.1	−24.1	−26.0	−22.0	−30.3	−26.1	−26.0
$OH^- + CH_3F \rightarrow HOCH_3 + F^-$	−20.3	−20.8	−20.8	−20.3	−20.4	−20.5	−20.1
$H + N_2 \rightarrow HN_2$	26.9	5.7	−1.5	−3.7	2.8	−3.1	3.8
$H + C_2H_4 \rightarrow CH_3CH_2$	−44.1	−39.6	−39.6	−40.4	−40.7	−41.9	−40.0
$HCN \rightarrow HNC$	16.4	14.3	13.9	5.0	12.8	13.9	15.3
MUE	8.5	2.5	4.1	6.0	1.4	2.0	

[a]See Table 7 for active space descriptions.

performs more similarly to the hybrid functionals (which are well-known[28,37] to be better for barrier heights than are local functionals) than to the local PBE functional.

The last set of data is composed of reaction energies and is given in Table 8. The lowest average error for this set is provided by M06-2X (1.4 kcal/mol) followed by B3LYP (2.0 kcal/mol) and CASPT2 (2.5 kcal/mol). The tPBE calculations have a lower average error, 4.1 kcal/mol, than CASSCF or PBE. There are two cases where PBE has the wrong sign for the energy of reaction; although tPBE also has the incorrect sign in these cases, the improvement is in the correct direction. For the $H + N_2O$ reaction, which has the most multireference character by either the *M* or *P* diagnostic, tPBE improves upon PBE by about 8 kcal/mol, but it still underperforms compared to the other methods.

The average errors over all the test data are given in Table 9. The first row of Table 9 is averaged over all 56 data of the earlier tables. In the next row, we average over only the 10 transition metal data in the TMABE10 subdatabase, and in the third row, we average over the other 46 data, which are labeled MGE46 for 46 main-group energies. The first row shows that, on average, CASPT2 and tPBE have similar errors (2.7 and 3.2 kcal/mol, respectively) and both outperform standard KS−DFT, with the exception of M06-2X. Of the three KS functionals, M06-2X has the lowest average error of 2.1 kcal/mol, then B3LYP with an average error of 3.9 kcal/mol, and finally PBE with an average error of 6.9 kcal/mol. The second row of Table 9 shows that tPBE is the best of all six methods tested for transition metal−ligand bond energies. The third row of Table 9 shows that tPBE is better than either PBE or B3LYP for main group energetics, although not quite as good as CASPT2. It will be interesting to see how the performance improves after we optimize a density functional, but the present performance is already very encouraging for an unoptimized first-generation on-top density functional.

Table 9. Average Mean Unsigned Errors (kcal/mol)

	CASSCF	CASPT2	tPBE	PBE	M06-2X	B3LYP
MUE(CE56)[a]	12.5	2.7	3.2	6.9	2.1	3.9
MUE(TMABE10)[b]	22.2	5.5	4.5	7.6	7.2	6.1
MUE(MGE46)[c]	10.5	2.1	2.9	6.7	1.0	3.4

[a]The mean unsigned errors averaged over all data in Tables 2−8 [b]The mean unsigned errors from the last row of Table 3. [c]The mean unsigned errors averaged over all data in Tables 2 and 4−8.

8. CONCLUSIONS

We tested the performance of MC−PDFT across a wide variety of cases. A main purpose of this work was to create a test suite against which further improvements of MC-PDFT (especially the use of more economical wave functions and better density functionals, which are not yet developed) could be tested and measured, but the results are of great interest in their own right. The results show that tPBE reduces the average error in CASSCF by a factor of 3 and that of PBE by a factor of 2. Averaging errors over al 56 data, we find that the performance of MC−PDFT is as good on the average as the much more expensive CASPT2. This indicates that the using a qualitatively correct wave function to represent the density and on-top density and calculate the kinetic energy already goes a long way toward improving density functional theory over the Kohn−Sham formulation, even without optimizing new density functionals.

For main group atomization energies, MC−PDFT is better than CASPT2. For transition metal atomization energies, many of which are highly multireference in character, MC−PDFT is the best of all six methods tested here. While the test sets are smaller for proton affinities and alkyl bond dissociation energies, previous work has shown that these are still representative of larger databases; for these two subdatabases, MC−PDFT again has the best performance of all the methods tested. MC-PDFT also gives a reasonably accurate energy for the dimerization energy of water. Finally, for energies of reactions and barrier heights, MC−PDFT has a performance quality between that of the most (CASPT2 and M06-2X) and least (CASSCF and PBE) accurate methods that are tested here.

■ ASSOCIATED CONTENT

Supporting Information

Absolute energies of various calculations with varying basis sets; Cartesian coordinates. This material is available free of charge via the Internet at http://pubs.acs.org.

■ AUTHOR INFORMATION

Corresponding Authors

*E-mail: gagliardi@umn.edu.
*E-mail: truhlar@umn.edu.

Notes

The authors declare no competing financial interest.

DOI: 10.1021/ct5008235
J. Chem. Theory Comput. XXXX, XXX, XXX−XXX

■ ACKNOWLEDGMENTS

The authors are grateful to Andy Luo, Dongxia Ma, Roberto Peverati, Haoyu Yu, and Wenjing Zhang for helpful assistance. Research is supported by the Inorganometallic Catalyst Design Center, an Energy Frontier Research Center funded by the U.S. Department of Energy, Office of Basic Energy Sciences, Division of Chemical Sciences under Award DE-SC0012702. R.K.C. thanks the National Science Foundation for a Graduate Research Fellowship under Grant No. 00039202.

■ REFERENCES

(1) Szabo, A.; Ostlund, N. S. *Modern Quantum Chemistry: Introduction to Advanced Electronic Structure Theory*; Macmillan: New York, 1982.
(2) Kohn, W. *Rev. Mod. Phys.* **1999**, *71*, 1253−1266.
(3) Roos, B. O.; Taylor, P. R.; Siegbahn, P. E. M. *Chem. Phys.* **1980**, *48*, 157−173.
(4) Schmidt, M. W.; Gordon, M. S. *Annu. Rev. Phys. Chem.* **1998**, *49*, 233−266.
(5) Andersson, K.; Malmqvist, P. A.; Roos, B. O.; Sadlej, A. J.; Wolinski, K. *J. Chem. Phys.* **1990**, *94*, 5483−5488.
(6) Shavitt, I. In *Methods of Electronic Structure Theory*; Schaefer, H. F. III, Ed.; Plenum: New York, 1977; pp 277−318.
(7) Goddard, W. A., III; Dunning, T. H., Jr.; Hunt, W. J.; Hay, P. J. *Acc. Chem. Res.* **1973**, *6*, 368−376.
(8) (a) Malmqvist, P.; Rendell, A.; Roos, B. J. *Chem. Phys.* **1990**, *94*, 5477−5482. (b) Malmqvist, P. Å.; Pierloot, K.; Shahi, A. R. M.; Cramer, C. J.; Gagliardi, L. *J. Chem. Phys.* **2008**, *128*, 204109. (c) Shahi, A. R. M.; Cramer, C. J.; Gagliardi, L. *Phys. Chem. Chem. Phys.* **2009**, *11*, 10964−10972.
(9) Ivanic, J. *J. Chem. Phys.* **2003**, *119*, 9364−9376.
(10) Ma, D.; Li Manni, G.; Gagliardi, L. *J. Chem. Phys.* **2011**, *135*, 044128/1−11.
(11) (a) Li Manni, G.; Aquilante, F.; Gagliardi, L. *J. Chem. Phys.* **2011**, *134*, 034114/1−4. (b) Li Manni, G.; Ma, D.; Aquiliante, F.; Olsen, J.; Gagliardi, L. *J. Chem. Theory Comp.* **2013**, *9*, 3375−3384.
(12) Hohenberg, P.; Kohn, W. *Phys. Rev.* **1964**, *136*, B864−B871.
(13) Kohn, W.; Sham, L. J. *Phys. Rev.* **1965**, *140*, A1133−A1138.
(14) Schultz, N. E.; Zhao, Y.; Truhlar, D. G. *J. Phys. Chem. A* **2005**, *109*, 11127−11143.
(15) Jacob, C. R.; Reiher, M. *Int. J. Quantum Chem.* **2012**, 3661−3684.
(16) Li Manni, G.; Carlson, R. K.; Luo, S.; Ma, D.; Olsen, J.; Truhlar, D. G.; Gagliardi, L. *J. Chem. Theory Comput.* **2014**, *10*, 3669−3680.
(17) Moscardo, F.; San-Fabian, E. *Phys. Rev. A* **1991**, *44*, 1549−1553.
(18) Becke, A. D.; Savin, A.; Stoll, H. *Theor. Chim. Acta* **1995**, *91*, 147−156.
(19) Perdew, J. P.; Savin, A.; Burke, K. *Phys. Rev. A* **1995**, *51*, 4531−4541.
(20) Perdew, J. P.; Ernzerhof, M.; Burke, K.; Savin, A. *Int. J. Quantum Chem.* **1997**, *61*, 197−205.
(21) Gräfenstein, J.; Cremer, D. *Mol. Phys.* **2005**, *103*, 279−308.
(22) Perdew, J. P.; Burke, K.; Ernzerhof, M. *Phys. Rev. Lett.* **1996**, *77*, 3865−3868.
(23) Becke, A. D. *Phys. Rev. A* **1988**, *38*, 3098−3100.
(24) Lee, C.; Yang, W.; Parr, R. G. *Phys. Rev. B* **1988**, *37*, 785−789.
(25) Becke, A. D. *J. Chem. Phys.* **1993**, *98*, 5648−5652.
(26) Stephens, P.; Devlin, F. J.; Chabalowski, C. F.; Frisch, M. J. *J. Phys. Chem.* **1994**, *98*, 11623−11627.
(27) Zhao, Y.; Truhlar, D. G. *Theor. Chem. Acc.* **2007**, *120*, 215−241.
(28) Zhang, W.; Truhlar, D. G.; Tang, M. *J. Chem. Theory Comput.* **2013**, *9*, 3965−3977.
(29) Zhao, Y.; Schultz, N. E.; Truhlar, D. G. *J. Chem. Theory Comput.* **2006**, *2*, 364−382.
(30) Zhang, W.; Truhlar, D. G.; Tang, M. *J. Chem. Theory Comput.* **2014**, *10*, 2399−2409.
(31) Zhao, Y.; Truhlar, D. G. *J. Phys. Chem. A* **2006**, *110*, 10478−10486.
(32) Zhao, Y.; Truhlar, D. G. *J. Chem. Phys.* **2006**, *125*, 194101/1−18.
(33) Izgorodina, E. I.; Coote, M. L.; Radom, L. *J. Phys. Chem. A* **2005**, *109*, 7558−7566.
(34) Zhao, Y.; Truhlar, D. G. *J. Chem. Theory Comput.* **2005**, *1*, 415−432.
(35) Zhao, Y.; Lynch, B. J.; Truhlar, D. G. *Phys. Chem. Chem. Phys.* **2005**, *7*, 43−52.
(36) Zhao, Y.; González-García, N.; Truhlar, D. G. *J. Phys. Chem. A* **2005**, *109*, 2012−2018.
(37) Zheng, J.; Zhao, Y.; Truhlar, D. G. *J. Chem. Theory Comput.* **2009**, *5*, 808−821.
(38) Peverati, R.; Truhlar, D. G. *Philos. Trans. R. Soc. A* **2014**, *372*, 20120476/1−51.
(39) Noodleman, L. *J. Chem. Phys.* **1981**, *74*, 5737−5743.
(40) Yamaguchi, K.; Jensen, F.; Dorigo, A.; Houk, K. N. *Chem. Phys. Lett.* **1988**, *149*, 537−542.
(41) Cramer, C. J.; Truhlar, D. G. *Phys. Chem. Chem. Phys.* **2009**, *11*, 10757−10816.
(42) Luo, S. J.; Averkiev, B.; Yang, K. R.; Xu, X. F.; Truhlar, D. G. *J. Chem. Theory Comput.* **2014**, *10*, 102−121.
(43) Aquilante, F.; De Vico, L.; Ferré, N.; Ghigo, G.; Malmqvist, P.-Å.; Pedersen, T.; Pitonak, M.; Reiher, M.; Roos, B. O.; Serrano-Andrés, L.; Urban, M.; Veryazov, V.; Lindh, R. *J. Comput. Chem.* **2010**, *31*, 224−247.
(44) Weigend, F.; Ahlrichs, R. *Phys. Chem. Chem. Phys.* **2005**, *7*, 3297−3305.
(45) Zheng, J.; Xu, X.; Truhlar, D. G. *Theor. Chem. Acc.* **2011**, *128*, 295−305.
(46) Lynch, B. J.; Zhao, Y.; Truhlar, D. G. *J. Phys. Chem. A* **2003**, *107*, 1384−1388.
(47) Forsberg, N.; Malmqvist, P.-Å. *Chem. Phys. Lett.* **1997**, *274*, 196−204.
(48) Ghigo, G.; Roos, B. O.; Malmqvist, P. Å. *Chem. Phys. Lett.* **2004**, *396*, 142−149.
(49) Lee, T. J.; Taylor, P. R.; Int, J. *Quantum Chem. Symp.* **1989**, *23*, 199−207.
(50) Lee, T. J.; Rendell, A. P.; Taylor, P. R. *J. Phys. Chem.* **1990**, *94*, 5463−5468.
(51) Heard, G. L.; Marsden, C. J.; Scuseria, G. E. *J. Phys. Chem.* **1992**, *96*, 4359−4366.
(52) Gordon, M. S.; Schmidt, M. W.; Chaban, G. M.; Glaesemann, K. R.; Stevens, W. J.; Gonzalez, C. *J. Chem. Phys.* **1999**, *110*, 4199−4207.
(53) Schultz, N. E.; Zhao, Y.; Truhlar, D. G. *J. Phys. Chem. A* **2005**, *109*, 11127−11143.
(54) Zheng, J.; Zhao, Y.; Truhlar, D. G. *J. Phys. Chem. A* **2007**, *111*, 4632−4642.
(55) Tishchenko, O.; Zheng, J.; Truhlar, D. G. *J. Chem. Theory Comput.* **2008**, *4*, 1208−1219.
(56) Timerghazin, Q. K.; Peslherbe, G. H.; English, A. M. *Phys. Chem. Chem. Phys.* **2008**, *10*, 1532−1539.
(57) Zhao, Y.; Tishchenko, O.; Gour, J. R.; Li, W.; Lutz, J. J.; Piecuch, P.; Truhlar, D. G. *J. Phys. Chem. A* **2009**, *113*, 5786−5799.
(58) Mintz, B.; Chan, B.; Sullivan, M. B.; Buesgen, T.; Scott, A. P.; Kass, S. R.; Radom, L.; Wilson, A. K. *J. Phys. Chem. A* **2009**, *113*, 9501−9510.
(59) Hajgató, B.; Szieberth, D.; Geerlings, P.; De Proft, F.; Deleuze, M. S. *J. Chem. Phys.* **2009**, *31*, No. 224321.
(60) Oyedepo, G. A.; Peterson, C.; Wilson, A. K. *J. Chem. Phys.* **2011**, *135*, No. 094103.
(61) Jiang, W.; Deyonker, N. J.; Determan, J. J.; Wilson, A. K. *J. Phys. Chem. A* **2012**, *116*, 870−885.
(62) Jiang, W.; Deyonker, N. J.; Wilson, A. K. *J. Chem. Theory Comput.* **2012**, *8*, 460−468.
(63) Law, M. M.; Fraser-Smith, J. T.; Perotto, C. U. *Phys. Chem. Chem. Phys.* **2012**, *14*, 6922−6936.

DOI: 10.1021/ct5008235
J. Chem. Theory Comput. XXXX, XXX, XXX−XXX

(64) Boguslawski, K.; Tecmer, P.; Barcza, G.; Legeza, O.; Reiher, M. *J. Chem. Theory Comput.* **2013**, *9*, 2959−2973.
(65) Fogueri, U. R.; Kozuch, S.; Karton, A.; Martin, J. M. L. *Theor. Chem. Acc.* **2013**, *132*, 1−9.
(66) Torres, A. E.; Guadarrama, P.; Fomine, S. *J. Mol. Modeling* **2014**, *20*, No. 2208.
(67) Hill, J. G.; Bucher, G. *J. Phys. Chem. A* **2014**, *118*, 2332−2343.
(68) Zhao, Y.; Truhlar, D. G. *J. Phys. Chem. A* **2008**, *112*, 1095−1099.
(69) Yang, K.; Zheng, J.; Zhao, Y.; Truhlar, D. G. *J. Chem. Phys.* **2010**, *132*, 164117/1−10.
(70) Steinmann, S. N.; Wodrich, M. D.; Corminboeuf, C. *Theor. Chem. Acc.* **2010**, *127*, 429−442.

DOI: 10.1021/ct5008235
J. Chem. Theory Comput. XXXX, XXX, XXX−XXX